JOURNAL OF SOLID STATE CHEMISTRY 34, 137–147 (1980)

Studies of Layered Uranium(VI) Compounds. III. Structural Investigations of Hydrogen Uranyl Phosphate and Arsenate Tetrahydrates below the Respective Transition Temperatures of 274 and 301°K

MARK G. SHILTON* AND ARTHUR T. HOWE

Department of Inorganic and Structural Chemistry, University of Leeds, Leeds LS2 9JT, England

Received March 20, 1979; in revised form August 6, 1979

The layered hydrates $HUO_2PO_4 \cdot 4H_2O$ (HUP), and $HUO_2AsO_4 \cdot 4H_2O$ (HUAs), which are proton-conducting solid electrolytes above the conductivity transitions at 274 and 301°K, respectively, have been shown, using powder X-ray diffraction, to change from tetragonal to orthorhombic symmetry below these temperatures. For HUP the unit-cell dimensions were $a = 6.985(5)$ and $c = 17.45(1)$ Å at 290°K, and $a = 6.966(5)$, $b = 7.004(5)$, and $c = 17.43(1)$ Å at 260°K. The values for HUAs were $a = 7.150(2)$ and $c = 17.608(5)$ Å at 305°K, and $a = 7.128(2)$, $b = 7.168(2)$, and $c = 17.613(5)$ Å at 293°K. The enthalpies of these displacive-type transitions were found from differential scanning calorimetry to be less than 0.5 kJ per mole of water for both compounds. Such a small value indicates that the rigid-like water lattices existing below the transitions do not become liquid-like above the transitions. The infrared spectra of HUP and HUAs both above the transitions, and down to 80°K, showed clear evidence of the presence of H_3O^+ ions, showing that the conductivity transitions are not caused by a loss of carriers. Rather, the antiferroelectric ordering, known to exist for HUAs, would appear to cause the conductivity drop. Upon this indication of ordering within the water layers, two possible related H-bond ordered structures have been proposed which are consistent with the observed twinning behavior and cell symmetry. The same ordered structures are suggested for HUP from our observations of the twinning behavior.

Introduction

We have recently established (*1, 2*) that the layered hydrate hydrogen uranyl phosphate tetrahydrate, $HUO_2PO_4 \cdot 4H_2O$ (HUP), has a high proton conductivity, which is in the region of solid electrolyte interest (*3*). Both the conductivity (*1*) and NMR relaxation times (*4*) show a sudden decrease below 274°K. In the isostructural arsenate (HUAs), the conductivity (*5*) and NMR discontinuities (*4*) coincide with the previously reported paraelectric–antiferroelectric transition in the region of 291–301°K (*6–8*). We have undertaken a study of the nature of the transitions in both HUAs and HUP in order to elucidate the reasons for the conductivity and NMR changes. Further aspects relating to the conductivities of HUP and HUAs will be presented in Part IV (*5*).

HUAs and possibly also HUP appear to have unusual dielectric properties. Of the small number of hydrates which exhibit dielectric ordering (*9*), most are ferroelectric. The only reported antiferroelectric hydrates, apart from HUAs, are $(NH_2CH_2COOH)_2H_2SO_4 \cdot H_2O$ and

* Present address: The Radiochemical Centre, Amersham, Buckinghamshire, U.K.

0022-4596/80/110137-11$02.00/0

$Cu(HCOO)_2 \cdot 4H_2O$ (CFT), the properties of which have been tabulated (*9*). CFT possesses sheets of water molecules, as are also found in HUP and HUAs, and ordering of the H bonds occurs in the antiferroelectric phase (*10, 11*) producing a doubling of the *c* axis (*12*). It was not known for HUP or HUAs whether ordering occurred in the water network or in the structural framework of the $(UO_2P/AsO_4)_n^{n-}$ layers. We have used X-ray diffraction, ir spectroscopy, differential scanning calorimetry (DSC), and optical microscopy to study the transitions of HUAs, the deuterated form (DUAs), and HUP. As a result of these studies we have been able to propose H-bond ordered structures (*13*), and these will be discussed here in the context of the above measurements. Studies of the dehydration behavior and phase relationships of HUP and HUAs have been reported in Part II (*14*).

Several uranium mica minerals were found in the 1870s near Schneeberg in Germany (*15*). Among these were troegerite, $HUO_2AsO_4 \cdot 4H_2O$ (HUAs), and uranospinite, $Ca(UO_2)_2(AsO_4)_2 \cdot nH_2O$. These are members of the wider class of uranium mica minerals of general formula $A^{z+}(UO_2XO_4)_z \cdot nH_2O$, where *A* may be almost any monovalent or divalent cation, *X* may be P or As, and *n* can range from 2 to 8. While the X-ray reports showed troegerite to have tetragonal symmetry (*15*), morphological and optical studies showed biaxial properties only consistent with a lower symmetry (*15, 16*). Uranospinite minerals, and the related phosphate minerals autunite and torbenite, showed variously uniaxial or biaxial character. Such changes from uniaxial to biaxial character, even observable as different zones within single crystallites, have been attributed to variations in the water content of troegerite (*16–18*) and other uranium micas (*15, 17–19*), or alternatively due to strain (*15*). Synthetic preparations of HUAs by Mrose (*20*), referred to as synthetic hydrogen uranospinite, were found to be tetragonal, and were uniaxially negative in contrast to troegerite.

de Benyacar and co-workers, in a series of papers on HUAs (*6–8*), initially referred to as synthetic troegerite, but later called hydrogen uranospinite, identified two transitions. Above about 291°K HUAs was uniaxial and paraelectric (phase I); at lower temperature it was biaxial and antiferroelectric (phase II), and below about 253°K it was still biaxial but now ferroelectric (phase III). The presence of the transition at a temperature in the ambient range which was found to vary from batch to batch of crystals explains many of the earlier apparent inconsistencies. However, careful Weissenberg photographs of phase II still revealed only a tetragonal unit cell, in conflict with the optical data.

The properties of HUP have been reviewed in Part I (*2*). Neither birefringence nor dielectric ordering has been reported for HUP.

Experimental

HUP and HUAs were prepared by precipitation from equimolar solutions of uranyl nitrate and phosphoric or arsenic acids, respectively, as previously described (*14*). The compositions were confirmed by chemical analysis and TGA. X-Ray data were obtained with a Philips PW 1050/25 powder diffractometer having a variable temperature stage, and using Cr radiation ($\lambda = 2.291$ Å), and $KAl(SO_4)_2 \cdot 12H_2O$ as a standard ($a = 12.158$ Å). Care was taken to maintain precisely the same sample heights in the holder, since the low-angle peaks were sensitive to this. A Perkin–Elmer DSC 1B instrument was used to obtain the DSC data, and the ir spectra were recorded on a Perkin–Elmer 457 instrument.

Results

X-Ray and Optical Studies

HUAs. Crystallites of HUAs from

various batches all showed biaxial character under the polarizing microscope at room temperature (290–293°K) if examined soon after filtration. Platelets up to about the average size of 1 μm usually were single domain. The larger crystals often showed twinning along the {110} planes producing platelets containing two or more domains. Still larger crystals, of about 0.2 mm in size and grown from their equilibrium solution, showed the characteristic striae of pencil-shaped domains, about 1 μm wide, and extending across the platelets, as have been described in detail by de Benyacar and co-workers (*6*, *7*). (We could not tilt the microscope stage in order to observe the subdomains described by de Benyacar and co-workers.) The biaxial character was no longer evident in crystals about 1 mm wide, and 0.1 mm thick, which is an expected optical consequence for thick crystals. Weissenberg photographs of such crystals, taken by Dr. W. S. McDonald, showed diffuse spots consistent with twinning. Our powder X-ray studies should have been able to identify the lower-symmetry cell demanded by the birefringence.

We found that precipitate which had been separated from the supernatant liquid, but not washed, gradually became uniaxial over the period of a day or so if left on the microscope slide in the laboratory. This was accompanied by the appearance of sometimes several new 002 peaks at lower angles in the X-ray pattern. These changes were found to be due to reaction with atmospheric NH_3 to produce the NH_4^+-substituted form. Precipitate which had been washed to pH 2 and dried in air took about 1 to 4 weeks to show evidence of reaction with NH_3. All NH_3 solutions and stock bottles were henceforth excluded from the laboratory. The washed and unwashed precipitates showed the same optical and X-ray properties initially.

The sample of HUAs used for the X-ray work had been stored with its equilibrium solution for 18 months in a sealed container, and was filtered, washed in arsenic acid of pH 2 until the filtrate was pH 1.8, and dried in air at 295°K for 24 hr. The X-ray diffractogram at 293°K of this biaxial HUAs powder was similar to that tabulated by Mrose (*20*) for uniaxial material, with the exception that reflections for which $h \neq k$ were broadened and many were split into well-resolved doublets. This had not been previously observed, and indicated an orthorhombic unit cell, which would explain the biaxial character of HUAs in the antiferroelectric phase II. Weissenberg photographs taken on larger single crystals, which would possess multiple domains of orthorhombic symmetry, would be expected to show an apparent tetragonal unit cell, with possible spot broadening, as indeed found by both ourselves and earlier workers, and this has hitherto prevented the true symmetry from being determined.

The lattice parameters at 293°K, calculated using all the major peaks, were $a = 7.128(2)$, $b = 7.168(2)$, and $c = 17.613(5)$ Å, where the errors in the last digits are indicated in parentheses. A 121 peak, observed by both ourselves and Mrose (*20*), is forbidden for a unit cell having half this c dimension, and confirms the double cell, representing two complete structural layers, as reported by Walenta (*17*, *18*). Mrose (*20*) failed to assign the 121 peak.

The temperature dependence of the lattice parameters, extending up into tetragonal phase I, was conveniently obtained by observing just selected high-angle peaks using the diffractometer hot stage. The results, illustrated in Fig. 1, clearly show the sharp transition at approximately 301°K to the tetragonal phase. There is a noticeable expansion in the a–b plane, and a possible slight contraction in the c direction to give a net volume expansion of $(0.05 \pm 0.01)\%$ in going to the tetragonal phase. Above 320°K the c axis is seen to contract due to the onset of dehydration, which nevertheless leaves

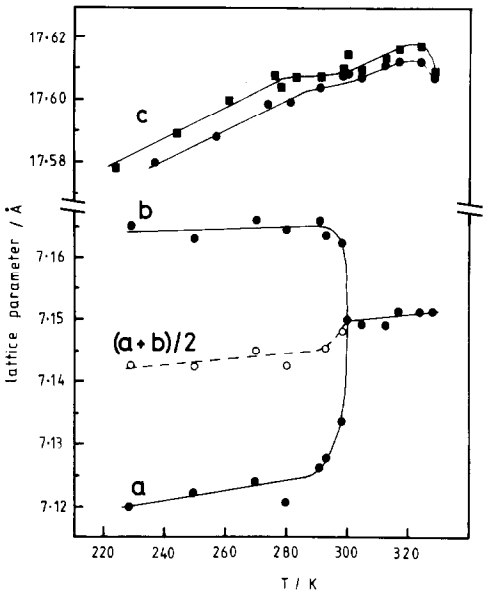

FIG. 1. Lattice parameters of HUAs, showing the change from the orthorhombic to the tetragonal high-temperature phase at 301°K. a and b were determined from the 310 and 130 peaks, the upper values of c from the 1, 1, 10 peaks, and the lower values of c from the unresolved 106 and 016 peaks. Absolute errors are ±0.01 Å; relative errors are much smaller than this.

the a axis unchanged. Small temperature changes are seen to alter the c parameter quite detectably over the entire temperature range studied, and the temperature of measurement should therefore be stated in accurate work. The coefficient of thermal expansion in the c direction was $(5 \pm 1) \times 10^{-4}\ K^{-1}$ and the average of that in the a and b direction was $(3 \pm 1) \times 10^{-5}\ K^{-1}$.

A complete diffraction pattern of tetragonal HUAs was recorded at 305°K, and the lattice parameters were $a = 7.150(2)$ and $c = 17.608(5)$ Å. Previous determinations show a spread of values, of a from 7.10 to 7.16 Å, and of c from 17.50 to 17.60 Å (*20–23*), with our values and those of Mrose (*20*) being at the top ends of the ranges. The space group was identified as *P4/ncc*, which is derived from *P4/nmm* quoted by Mrose (*20*) by a doubling of the c parameter. The small changes in going from phase I to phase II indicate a displacive rather than a reconstructive transition. The space group for phase II will therefore be derived from *P4/ncc* found in phase I, indicating, in conjunction with the X-ray pattern, that the space group of highest allowable symmetry is *Pccn*.

The data did not reveal any changes across the reported phase II to phase III transition at 253°K (*7*). The observed phase I to phase II transition temperature of 301°K agrees with the maximum in the temperature range of 291 to 301°K observed by de Benyacar and de Abeledo (*6*) for different batches of crystals. We found that such variations in the transition temperature correlated with variations in the atmospheric humidity. For example, a sample of orthorhombic HUAs which was kept *in situ* on the diffractometer stage in a flowing saturated air/nitrogen mixture of water vapor pressure 5 mm Hg (0.7 kN m^{-2}) was tetragonal at 292°K the next day. Such a lowering of the transition temperature is probably due to a slight loss of water within the slightly nonstoichiometric tetrahydrate phase, which can be expressed more precisely as $HUO_2AsO_4 \cdot (4-x)H_2O$, where x is probably less than 0.05 (*14*). The slight water loss may also be accompanied by the loss of small amounts of a phosphorus-containing compound such as P_2O_5 or H_3PO_4 (*14*). The conductivity transition occurred at 301°K (*5*), and since the disk was immersed in solution this must represent the maximum transition temperature.

HUP. HUP exists in three crystallographic modifications (types I, II, and III) as described by Moroz *et al.* (*22*), and discussed in Part I (*2*). Our work relates to type I (*2*), which is tetragonal at ambient temperatures and for which a single-crystal X-ray study has recently been reported (*24*). So far there is only evidence of one modification of HUAs, which appears to correspond to the type I modification of HUP. We report, for the first time, the observation of optical birefringence and domain formation in HUP crystals below

about 274°K, thus confirming the presence of a crystallographic distortion similar to that found in HUAs. The optical characteristics were the same in all respects to those described by ourselves and by de Benyacar and de Abeledo (*6*) for HUAs.

At 290°K the lattice parameters were found to be $a = 6.985(5)$ and $c = 17.45(1)$ Å, with a space group consistent with $P4/ncc$. Our values do show a small, but experimentally significant, difference to those of $a = 6.995(2)$ and $c = 17.491(4)$ Å obtained from the single-crystal study (*24*). The differences may result from slightly different water contents within the nonstoichiometric tetrahydrate phase (*14*), arising from different atmospheric conditions.

Figure 2 shows the transition at 274°K to what was identified as an orthorhombic unit cell, of space group *Pccn*, deduced on the assumption of a displacive transition from

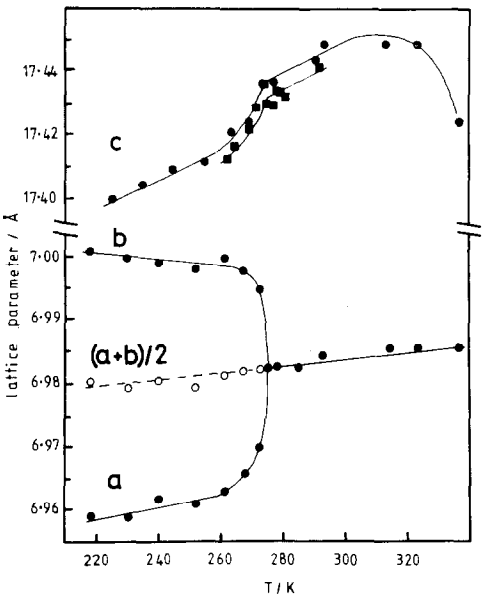

FIG. 2. Lattice parameters of HUP, showing the change from the orthorhombic to the tetragonal, high-temperature phase, at 274°K. *a* and *b* were determined from the 310 and 130 peaks, and *c* was determined from the 008 peak (the data for two separate runs are shown). Absolute errors are ±0.01 Å; relative errors are much smaller than this.

$P4/ncc$ found in phase I (*24*). The coefficients of thermal and volume expansion were the same as those for HUAs. The lattice parameters at approximately 260°K were $a = 6.966(5)$, $b = 7.004(5)$, and $c = 17.43(1)$ Å.

Differential Scanning Calorimetry (DSC)

Values for the enthalpies of the phase I to phase II transitions have not been reported for any of the compounds. We found the values to be so small that an accurate determination could not be made. However, an upper limit of 0.5 kJ per mole of water was established for all three compounds, HUAs, DUAs (93% deuterated), and HUP. The peaks were reasonably symmetrical, and spread over about 4°K at the slowest heating rate used of 1°K min^{-1}. Extrapolation of the leading edge of the peak (*25*) gave the transition temperatures as 299, 290, and 271°K for HUAs, DUAs, and HUP with an absolute uncertainty in the temperatures of 3°K. No peaks were detected for the phase II to phase III transition in HUAs, which is consistent with the lack of a peak in the DTA (*6*).

Infrared Spectra

Samples of HUAs and HUP were washed, to remove excess acid, until the equilibrium solutions were pH 2, filtered, dried between filter papers, and then air-dried. The powders were ground in the presence of Nujol, and pressed between AgCl disks. Spectra were recorded over a range of temperatures from 80 to 330°K in an evacuated cryostat. Only after several hours at the highest temperature were there any noticeable effects of dehydration or chemical change.

Representative spectra are shown in Fig. 3. As can be seen, there were only small differences between the three respective phases of HUAs and HUP. The three HUAs spectra clearly show the H_3O^+ asymmetrical and symmetrical bending modes at 1750 and

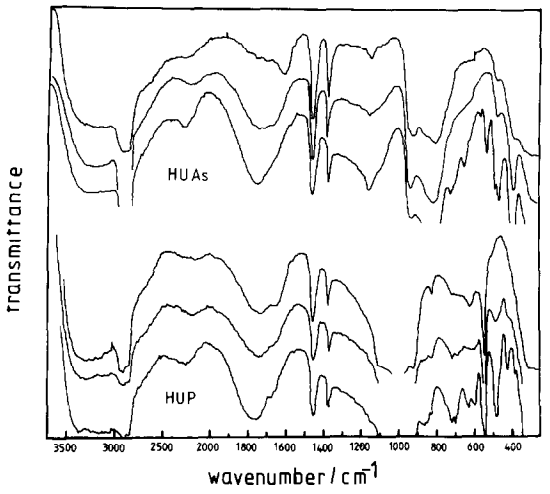

FIG. 3. Infrared spectra of HUAs and HUP, at temperatures covering the three possible phases of each. The temperatures for HUAs, from top to bottom, were 330, 293, and 80°K, and those for HUP, from top to bottom, were 293, approximately 250, and 80°K. The sharp peaks which occur at the same frequencies for both samples arise from Nujol.

1150 cm^{-1}, respectively, as previously assigned for the room temperature spectrum (*26*). These peaks intensified at the lower temperatures, and there were also intensity changes in the two water bands in the region of 3400 and 1620 cm^{-1}. In HUP, only the H_3O^+ peak at 1750 cm^{-1} is resolved, as previously assigned for the room temperature spectrum (*22, 27*), and again the peak intensified at lower temperatures.

The ir spectra clearly show that the H_3O^+ ions are present in all three phases despite the antiferro- and ferroelectric ordering known to exist in HUAs. Moreover, the widths of the H_3O^+ and H_2O peaks at 80°K indicate that the ordering has not resulted in unique sites for these species within the H-bonded network. One further point is that the single-crystal study of HUP (*24*) revealed very short H bonds (2.56 Å) linking oxygens in adjacent water squares, suggestive of the possible presence of $H_5O_2^+$ ions. However, although spectra of both HUP and HUAs showed peaks in the 2200 to 2300 cm^{-1} region expected for $H_5O_2^+$ (*28*), the possible presence of water bands also in this region prevents a definite assignment from being made.

Discussion

The X-ray results have established that the paraelectric–antiferroelectric transition observed in HUAs is accompanied by a displacive transition which results in orthorhombic symmetry. A similar transition has been shown to occur in HUP, and it is likely that HUP also becomes antiferroelectric, although this has not yet been specifically confirmed.

The ordering responsible for the antiferroelectricity could occur in the uranyl–phosphate layers, the water layers, or possibly in both. However, the large changes in both the H^+ conductivity (*1, 2, 5*) and NMR relaxation times (*4*) in both HUP and HUAs at the transition temperatures, would indicate a significant change in the water behavior through the transition. The possibility that this could be due to a "freezing" of the waters between the layers can be ruled out since the observed enthalpies of transition of less than 0.5 kJ per mole of water are far too low compared to the enthalpy of freezing of ice of 4.8 kJ $mole^{-1}$, for example. The hydrogen-bonded water network is therefore essentially solid-like both above and below the transition. This accords with activation energies for both HUP and HUAs for the spin lattice and spin–spin relaxation times of 20 kJ $mole^{-1}$ above the transition, and values higher than this below the transition (*4*). The very small dimensional changes occurring at the transition would not themselves be expected to drastically alter the behavior of the water molecules either. We therefore infer that at least ordering of the H bonds within the water structure occurs in going to the antiferroelectric phase. The ordering would inhibit H^+ conductivity, causing a sudden drop in the conductivity as

observed. The ir results show that the conductivity transition could not be caused by proton trapping on basic sites of the $(UO_2PO_4)_n^{n-}$ layers, since H_3O^+ was still present at low temperatures.

On the basis of the X-ray and twinning data, we have been able to propose an ordered H-bond scheme which explains the antiferroelectric properties. A definitive determination of the H (or D) positions in the compounds by X-ray or neutron diffraction, which is being tried by Dr. B. E. F. Fender of Oxford, will be extremely difficult due to the complex twinning behavior of the crystals in the antiferroelectric phase. de Benyacar and de Dussel (*8*) recognized that the twinning planes could not be symmetry planes of the structure. The available evidence at the time indicated that the space group of the paraelectric phase was $P4/mmm$. Our evidence, for both HUAs and HUP, indicates a doubling of the c dimension to give the space group $P4/ncc$. Exclusion of the {110} and $\{1\bar{1}0\}$ domain planes, and {100} and {010} subdomain planes as symmetry planes reduces the point group of $4/mmm$, which is common to both space groups $P4/mmm$ and $P4/ncc$, to either one of the point groups, 1, $\bar{1}$, 2 or 222 (*8*). Only 222 is consistent with our findings of orthorhombic symmetry, giving a space group of $P2_12_12$. This is of lower symmetry than that deduced directly from the X-ray data, but would not be experimentally distinguishable using our data from *Pccn* because the observed reflections are consistent with both space groups. We therefore looked for ordered structures having the space group $P2_12_12$.

The structure of HUP, as obtained from a single-crystal study of the paraelectric phase (*24*), has been fully described in Part I (*2*). The water molecules in this phase occupy a unique position, and are arranged in squares which are linked to each other at each corner, as shown in Fig. 4, to form a continuous puckered network. The two square (s) H bonds and one link (l) H bond associated

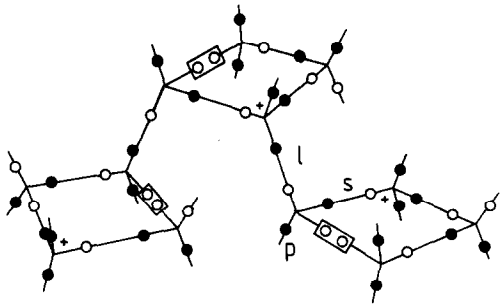

FIG. 4. H-Bond network in HUP or HUAs, showing a possible arrangement conforming to the suggested ordered structure. The oxygens at the intersections of the lines are not shown. Filled H-bond positions, ●; unfilled positions, ○; H-bond vacancies are signified by a rectangle. p bonds point up and down to phosphate groups, l bonds link neighboring squares of water molecules, and s bonds link water molecules within each square.

with each water are shown in the figure. The fourth H bond belonging to each oxygen is to an oxygen of a phosphate or an arsenate group either in the $(UO_2XO_4)_n^{n-}$ layer above, or in a similar layer below. These H bonds are labeled p in Fig. 4. The unit cell contains two water layers, and two $(UO_2XO_4)_n^{n-}$ layers, in which the XO_4^{3-} groups are twisted slightly relative to each other.

For every four water molecules there are 10 potential H bonds. However, there are only nine protons, leaving an H-bond vacancy. Each square, then, contains one H_3O^+ ion and one H-bond vacancy, as shown in Fig. 4. Whether the vacancies are on the link, square, or phosphate sites does not influence the deduction of the ordered structures. For the purposes of Fig. 4, we have assigned the vacancies to the square sites, which would aid water reorientation necessary for conduction in phase I (*2*). The short link distances found in phase I (*24*) of 2.56 Å would be inconsistent with vacancies in the link positions. The presence of H_3O^+ ions shows that the hydrogens in the phosphate bonds are, for all phases, on the water side of the bonds, and will not be further

considered regarding possible ordered structures. Bands due to P–O–H hydrogen bonds are not present in the appropriate region of the ir spectra. Such a band was identified at 2380 cm^{-1} for a dehydrated form of HUP (*22, 27*).

Taking the space group $P2_12_12$, we have tried to derive structures in which the order is produced by (a) assigning one H-bond dipole to each possible H bond and arranging these to suit, and allowing the H_3O^+ and vacancies to be incorporated where necessary in a nonordered fashion, (b) incorporating the H_3O^+ ions into the ordered dipole arrangement in an ordered way, with the vacancies not ordered, (c) incorporating the vacancies into the ordered dipole arrangement in an ordered way, with the H_3O^+ ions not ordered, and (d) incorporating both H_3O^+ ions and vacancies into the ordered dipole arrangement in an ordered fashion. Only arrangements of type (a) were found to give the space group $P2_12_12$. The other arrangements led to lower symmetries, which, although they could not be ruled out, could not be substantiated by the available data, and we shall now describe the structures conforming to the space group $P2_12_12$.

We could construct only two ordered structures for which the unit cells matched the orthorhombic unit cell. One structure is shown in Fig. 5, and the other is obtained by rotation of one of the water layers by 90°. The arrows represent the electrostatic dipoles along the O–O axes due to the hydrogens being off-center. The hydrogens therefore are at the tail ends of the arrows. Each oxygen is associated with a hydrogen in the fourth H bond (not shown) to the phosphate or arsenate oxygens. The ordering has destroyed the fourfold symmetry axis, resulting in a unit cell in which the *a* and *b* axes are inequivalent.

The dipole ordering is seen to be head to tail around the squares, which is an electrostatically stable configuration. In addition, there are chains head to tail of alternate

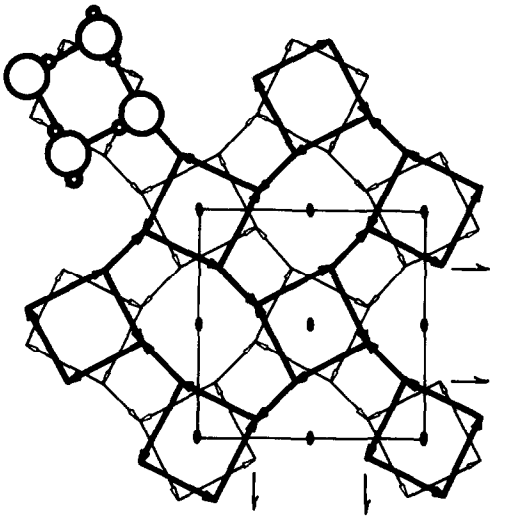

FIG. 5. One of the two suggested ordered structures in the two water layers (heavy and light lines) of HUP or HUAs. Large circles represent oxygens, small circles, hydrogens, which are at the positive, tail end of the arrows. Sheets of $(UO_2XO_4)_n^{n-}$ are interspaced between the illustrated water layers. The symmetry elements corresponding to $P2_12_12$ are indicated for the unit cell. (Half-arrows, twofold screw axes; ellipses, twofold rotation axes.) The sides of the square represent the *a* and *b* axes. We cannot, of course, determine which is which. The second proposed structure is obtained by rotation of one water layer through 90°.

link and square dipoles which run horizontally in Fig. 5, but not perpendicularly. The structures imply a coupling between successive water layers so as to provide for the correct interlayer dipole arrangement. Such a coupling is present in the few other dielectrically ordered layered hydrates such as CFT (*10*) already referred to, $SnCl_2 \cdot 2H_2O$ (*29, 30*), and $K_4Fe(CN)_6 \cdot 3H_2O$ (*31*).

Specification of the positions of H_3O^+ ions and vacancies in an unordered fashion does not alter the space group. There are only two positions within each square in the ordered structures which can accommodate a vacancy without producing an OH^- ion. These are in the positions shown in Fig. 4, and also on the opposite sides of each of the squares. As the structure is drawn in Fig. 5, each square contains two H_3O^+ ions, at the corners which

have two dipole tails, that is, two hydrogens, plus a third hydrogen in the phosphate H bond. The incorporation of one vacancy into each square leaves just one H_3O^+ ion, as required, and Fig. 4 shows the ordered dipole arrangement after a random incorporation of vacancies and H_3O^+ ions. Ordered arrangements of these entities not only lower the symmetry, but in many cases change the structure from being truly antiferroelectric to possessing a net dipole moment, which would then be inconsistent with the findings of antiferroelectricity by de Benyacar and de Dussel (*7*).

Although the atomic displacements caused by ordering are not necessarily prescribed by the space group of the ordered dipoles themselves, consideration of the likely dipole–dipole interactions in the ordered structures would suggest that the atomic displacements would conform to orthorhombic symmetry to retain the space group $P2_12_12$ in the relaxed structure. Whether displacements, which must occur also in the $(UO_2XO_4)_n^{n-}$ layers, are induced by the H-bond ordering, or whether there is an additional driving force from these layers we cannot tell.

Since the twinning directions were fed in to produce the deduced space group, the ordered structures will, of course, be consistent with the twinning behavior. However, many subtleties, itemized below, of the observed twinning behavior are well explained by the ordered structures, as will now be discussed.

1. The domain boundaries in both HUAs (*6*) and HUP (our observations) are visible using unpolarized light, indicating a structural discontinuity. The domain boundaries, along {110} or {1$\bar{1}$0}, result from the size difference between the *a* and *b* axes. Figure 6 shows a plan of two adjacent water layers in the structure. The mirror plane for the domain boundary (long line) exists after translation from one layer to the next, as shown. However, in the adjacent domains, all the dipole directions have been reversed compared to each other, as can be seen in Fig. 6, causing the *a* and *b* axes to be interchanged. This causes the domain boundary region to suffer considerable distortion, as is visually evident in the crystals.

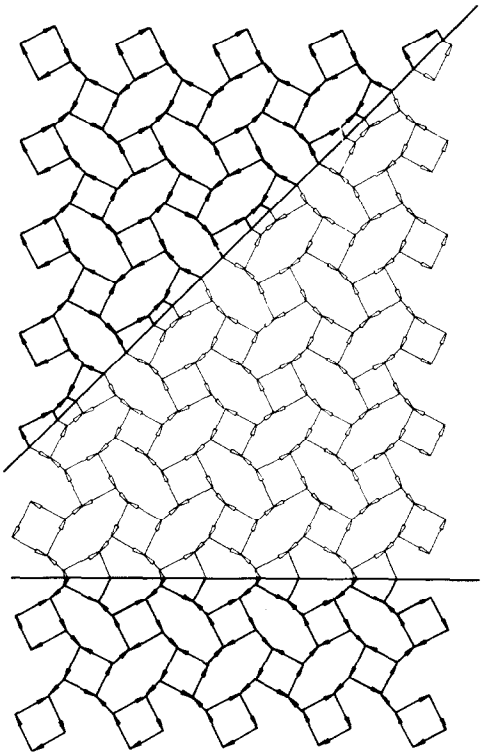

Fig. 6. Domain and subdomain boundaries (long and short lines, respectively) in one of the suggested structures, in which consecutive water layers (heavy and light lines) show mirror symmetry after translation to the next water layer, that is, by half a unit cell in the *c* direction, perpendicular to the layers.

2. The subdomain boundaries are not evident in unpolarized light (*6*). A subdomain boundary is shown in Fig. 6. It can be seen that across the boundary only the directions of the dipoles constituting the squares are reversed, which will leave the *a* and *b* axes unchanged becase of the fourfold symmetry of the square. Hence there will be little or no distortion associated with the subdomain boundaries, as observed.

3. The subdomains are not pencil shaped like the domains, but are much larger and cut across many domains (*6*). Large subdomains are possible in the proposed structures because they are not associated with stress relief. It can also be shown that the proposed domain and subdomain boundaries can intersect each other.

4. The subdomains were found to anneal out at lower temperatures, or upon temperature cycling (*6*). Since subdomains are not required to relieve stresses in the crystal, they are therefore free to anneal out to produce unisubdomain crystals.

It might be added that other related ordered structures can be generated by, for instance, reversing the dipole directions in every second water layer. These have a different symmetry and do not permit domain together with subdomain formation. This may provide another explanation of why subdomains were sometimes not observed (*6*).

In conclusion, we wish to emphasize that there is no immediately obvious way of producing an antiferroelectric ordered arrangement of the dipoles in the water network of HUP or HUAs. The structures which are suggested by the X-ray and twinning data are, in fact, some of the simplest ordered arrangements possible for this particular and unusual H-bond network: dipoles are head to tail around the squares, and along half of the zigzag dipole chains. Moreover, the unit cells of the ordered structures are identical to the dimensions of the basic orthorhombic unit cell, confirming the simplicity of the structures. We might add that satisfactory structures can be found in which the cell dimensions are multiples of the basic orthorhombic unit cell. Such a possibility may eventually be checked by neutron diffraction studies. However, the complete solution of an H-bond ordered structure is a formidable task, as can be seen from the literature on, for instance, $Cu(HCOO)_2 \cdot 4H_2O$ (*10–12*). While the complete solution of the structure is awaited, we feel that the presentation of one of the simplest ordered arrangements is of merit, particularly in view of the fact that it does afford a very satisfying explanation of the space group, the antiferroelectricity, the details of the twinning behavior, and the conductivity transition for compounds which are of considerable current interest as two of the few known proton-conducting solid electrolytes.

Acknowledgments

One of us, M.G.S., thanks the Science Research Council for a postdoctoral fellowship. We thank Dr. P. E. Childs for useful discussions, and Mr. J. Spencer and Mr. H. Hill for work in conjunction with the DSC and ir measurements.

References

1. M. G. SHILTON AND A. T. HOWE, *Mater. Res. Bull.* **12**, 701 (1977).
2. A. T. HOWE AND M. G. SHILTON, *J. Solid State Chem.* **28**, 345 (1979).
3. P. E. CHILDS, A. T. HOWE, AND M. G. SHILTON, *J. Power Sources* **3**, 105 (1978).
4. P. E. CHILDS, T. K. HALSTEAD, A. T. HOWE, AND M. G. SHILTON, *Mater. Res. Bull.* **13**, 609 (1978).
5. A. T. HOWE AND M. G. SHILTON, *J. Solid State. Chem.* **34**, 149 (1980).
6. M. A. R. DE BENYACAR AND M. E. J. DE ABELEDO, *Amer. Mineral.* **59**, 763 (1974).
7. M. A. R. DE BENYACAR AND H. L. DE DUSSEL, *Ferroelectrics* **9**, 241 (1975).
8. M. A. R. DE BENYACAR AND H. L. DE DUSSEL, *Ferroelectrics* **17**, 469 (1978).
9. LANDOLT-BÖRNSTEIN, "Ferro- and Antiferroelectric Substances," New Series III, Vol. 3, Springer-Verlag, Berlin/New York (1969); Vol. 9 (1975).
10. H. KIRIYAMA, *Bull. Chem. Soc. Japan* **35**, 1199, 1206 (1962).
11. M. KAY, *Ferroelectrics* **9**, 171 (1975).
12. K. C. TUBERFIELD, *Solid State Commun.* **5**, 887 (1967).
13. M. G. SHILTON AND A. T. HOWE, *Chem. Commun.*, 194 (1979).
14. A. T. HOWE AND M. G. SHILTON, *J. Solid State Chem.* **31**, 393 (1980).

15. C. H. PALACHE, H. BERMAN, AND C. FRONDEL, "System of Mineralogy of Dana," 7th ed., Vol. 2, p. 967, Wiley, New York (1966).
16. A. WEISS, F. TABORSZKY, K. HARTL, AND E. TROGER, *Z. Naturforsch. B* **12**, 356 (1957).
17. K. WALENTA, *Tschermaks Mineral. Petrogr. Mitt.* **9**, 111 (1964).
18. K. WALENTA, *Tschermaks Mineral. Petrogr. Mitt.* **9**, 252 (1965).
19. E. W. NUFFIELD AND I. H. MILNE, *Amer. Mineral.* **38**, 476 (1953).
20. M. E. MROSE, *Amer. Mineral.* **38**, 1159 (1953).
21. A. WEISS, K. HARTL, AND U. HOFFMANN, *Z. Naturforsch. B* **12**, 668 (1957).
22. I. KH. MOROZ, A. A. VALUEVA, G. A. SIDORENKO, L. G. ZHILTSOVA, AND L. N. KARPOVA, *Geokhim. USSR* **2**, 210 (1973).
23. F. WEIGEL AND G. HOFFMANN, *J. Less Common Metals* **44**, 99 (1976).
24. B. MOROSIN, *Phys. Lett. A.* **65**, 53 (1978).
25. J. L. MCNAUGHTON AND C. T. MORTIMER, *in* "International Review of Science" (A. D. Buckingham, Ed.), Ser. 2, Vol. 10, Chap. 1, Butterworths, London (1975).
26. R. W. T. WILKINS, A. MATEEN, AND G. W. WEST, *Amer. Mineral.* **59**, 811 (1974).
27. M. V. NIKANOVICH, G. G. NOVITSKII, L. V. KOBETS, T. A. KOLEVICH, V. V. SIKORSKII, AND D. S. UMREIKO, *Koord. Khim.* **2**, 253 (1976); *Coord. Chem.* (Russian) **2**, 192 (1976).
28. E. SCHWARZMANN, *Z. Naturforsch. B* **24**, 1104 (1969).
29. H. KIRIYAMA, H. KITAHAMA, O. NAKAMURA, AND R. KIRIYAMA, *Bull. Chem. Soc. Japan* **46**, 1389 (1977).
30. R. KIRIYAMA, H. KIRIYAMA, K. KITAHAMA, AND O. NAKAMURA, *Chem. Lett.*, 1105 (1973).
31. J. C. TAYLOR, M. H. MUELLER, AND R. Z. HITTERMAN, *Acta Crystallogr.* **26**, 559 (1970).